X_{CP}, since this flap is shielded at low α's but its effects become more prominent as α grows. Since there is no provision to account for this in the prediction method, X_{CP} comparisons were not made.

References

[1] Pitts, W. C., Nielsen, J. N., and Kaattari, G. E., "Lift and Center of Pressure of Wing-Body-Tail Combinations at Subsonic, Transonic and Supersonic Speeds," Rept. 1307, 1957, NACA.

[2] Allen, H. J., "Estimation of the Forces and Moments Acting on Inclined Bodies of Revolution," RM A9126, March 1951, NACA.

[3] Allen, H. J. and Perkins, E. W., "Characteristics of Flow Over Inclined Bodies of Revolution," RM A50L07, March 1951, NACA.

[4] Flax, A. H. and Lawrence, H. P., "The Aerodynamics of Low-Aspect-Ratio Wings and Wing-Body Combinations," Rept. CAL-37, Sept. 1951, Cornell Aeronautical Lab., Buffalo, N. Y.; also *Proceedings of Third Anglo-American Aeronautical Conference*, Brighton, England, Sept. 1951, London, Royal Aeronautical Society, 1952.

[5] Eaton, P. T., "A Method for Predicting the Static Aerodynamic Characteristics of Low-Aspect-Ratio Configurations," Rept. 2216, June 1966, David Taylor Model Basin, Washington, D. C.

[6] Gersten, K., "Calculation of Non-Linear Aerodynamic Stability Derivatives of Aeroplanes," Rept. 342, 1961, 1962, Advisory Group for Aeronautical Research and Development, Paris.

[7] Franz, G. E., "Lift Curve Slopes of Low Aspect Ratio Wings at Transonic Speeds," Applied Mechanics TN AM-TN-2-63, June 1963, North American Aviation, Columbus, Ohio.

[8] Douglas Aircraft Co., "USAF Stability and Control DATCOM," Rev. W-P AFB, June 1969, Vol. 2, Wright-Patterson Air Force Base, Ohio.

[9] Hoerner, S. F., *Fluid Dynamic Drag*, 2nd ed., Sighard F. Hoerner, Midland Park, N. J., 1958.

[10] Dommasch, D. O., Sherby, S. S., and Connolly, T. F., *Airplane Aerodynamics*, Pitman, New York, 1961.

[11] Beil, W. J. et al., "Major Developments for the Jet Vane Controlled Bomber Defense Missile," BE-754-S-24, March 1955, Cornell Aeronautical Lab., Buffalo, N. Y.

MAY 1971 J. SPACECRAFT VOL. 8, NO. 5

Recent Work on Radio Frequency Ion Thrusters

HORST W. LOEB*
University of Giessen, West Germany

Based on demonstration of feasibility and on careful optimizations, the standardized 10-cm-diam radio frequency ion thruster RIT 10 of 100 ma, 1.1 kg, 309 w, and 71.5% thruster efficiency, equipped with power conditioning and control units, has reached laboratory prototype maturity. Two advanced concept definition studies are under way in preparation for space testing of an rf-engine-cluster by spiralling up a 350 kg-satellite, probably in 1976. Measurements on plasma diagnostics, ion extraction and focusing mechanism, beam distribution, etc. have been performed. Variation of ionizer's diameter from 4 to 20 cm, considering scaling laws and optimization of all the parameters, has been accomplished. A large vacuum test facility of 28 m³ volume is in operation.

Introduction

TEN years ago, there were two main types of electrostatic engines: the cesium contact drive and Kaufman's mercury bombardment thruster. However, the former type has the disadvantage that it cannot use mercury as the propellant, and the latter type suffered in the beginning from lifetime problems due to discharge cathode erosion. Therefore, we began at the Giessen University to examine,[1] optimize,[2] and prove the feasibility of use[3] of the rf ion source for electrostatic propulsion purposes. Basic plasma and beam diagnostic measurements have been undertaken. A new extraction and focusing mechanism has been applied. Lifetime runs and a 11,000 ignition test have been carried out.[4] Auxiliary components—vaporizer, isolator, fully transistorized rf-transmitter, plasma bridge neutralizer, power conditioning, and thruster control unit—have been developed. The standardized 10-cm-diam rf-engine is now being prepared by the industry for flight qualification. Besides RIT 10, a small 4-cm-diam thrust unit for attitude control and station-keeping, and 20-cm-diam engines for main propulsion missions are under optimization. In total, a team of 18 scientists is working on rf-electric propulsion at six test stands and two computers.

The rf-ion source works with an electrodeless, annular, self-sustaining discharge and produces a dense, nonisothermal, quasi-neutral mercury plasma. Some advantages in respect to the other ion engine types are: 1) with no dischange electrodes, lifetime problems are avoided; 2) because of an ion optical focusing effect, very high propellant efficiencies have been gained; 3) owing to the rf-discharge electrons' Maxwell distribution, only singly charged Hg^+ ions are observed, resulting in a beam homogeneity of 100%; 4) the rf-ion source is easy to assemble and control. From the beginning, the following objections arose: 1) It is more difficult to couple the discharge energy electrodelessly from the outside into the plasma than to display it inside by d.c. electrodes. 2) A spontaneous breakdown of the rf-discharge is possible only by increasing pressure or using a special igniter electrode. 3) To the usual electrostatic beam spreading a focusion aperture is added, causing a divergence efficiency drop of about 1%. 4) In the case of poor shielding some harmonics of the rf-transmitter could possibly disturb the

Presented as Paper 70-1102 at the AIAA 8th Electric Propulsion Conference, Stanford, Calif., August 31–September 2, 1970; submitted October 27, 1970; revision received December 30, 1970. This report is dedicated to W. Hanle on the occasion to his 70th birthday. The author thanks all his co-workers for assistance. This research is supported by the German Ministry of Education and Science (Contract RFF 3034).

* Professor, Head of Electric Propulsion Department, 1st Institute of Physics. Member AIAA.

telemetry. 5) Because of the insulating discharge vessel, mechanical problems were feared.

As reported earlier,[4] all these disadvantages and problems have been removed or reduced to insignificance.

Operating Principles

In an rf-ion engine (Fig. 1) a pressurized gas feed system transports the liquid mercury via a valve into the vaporizer. A fine-meshed steel grid evaporates the propellant. An isolator separates the grounded boiler system and the ionizer's entrance.

The propellant vapor streams through the extracting anode into the ion source. The ionizer vessel is made of an insulating material and is positioned inside the induction coil of an rf-transmitter. According to the induction law, a high frequency electrical eddy field $\mathbf{E}_{ind}$ is induced, which accelerates the discharge electrons to gather ionization energy. They suffer elastic collisions with neutral Hg atoms in time with the rf-field, and move to and fro, gaining energy by this accumulation mechanism. The statistics can be affected in a favorable manner by adaption of the discharge pressure, i.e., the mean free flighttime, to the transmitter frequency. The Ramsauer effect aids the accumulation process.

By the skin effect, the conductive discharge plasma hinders the penetration of rf-energy into the interior regions of the ionizer. However, a weak, constant, perpendicular, magnetic field **H** compensates this partly by a resonance phenomenon.[5] Because of the induction law properties, the skin effect, the magnetic resonance effect, and the ambipolar diffusion, a radial plasma density decrease occurs.

To start the rf-discharge with low pressures, it is necessary to inject electrons from the filament of a grounded igniter, which is located inside the extraction anode cylinder, emitting electrons through the anode grid into the plasma.[4] Ion extraction from the discharge plasma is accomplished by a perforated isolator plate, called a plasma boundary anchor, and the extraction cathode. The extracting anode gathers electrons, to maintain the plasma's quasi-neutrality. For this, the plasma assumes automatically nearly anode potential.[6]

The potential of the anode stipulates the engine's specific impulse. The extracting cathode possesses a negative bias voltage, firstly to rise the extraction voltage, i.e., the potential difference between anode and cathode, using the accel-decel technique, and secondly to prevent the neutralizer electrons from streaming back and hitting the ion source.

As the plasma assumes anode potential and as there is formed a positive space charge in front of the extraction cathode, i.e., inside the plasma boundary holes, the total extraction voltage drops along the space charge region. The boundary between this region and the plasma, is anchored on the upper side of the aforementioned plasma boundary anchor.

Due to the shadow effect of the ion-absorbing plasma boundary, there is built up between this boundary sheath and the undisturbed plasma a transition region of disturbed plasma with a penetrating field.

The extractable ion current density is limited on one hand by yield of the discharge plasma, i.e., the plasma density and the transition field, on the other hand by a modified Langmuir-Schottky's $V^{3/2}$ law. In order to achieve high beam currents, both conditions, the plasma saturation and the space charge limitation, are to be optimized.

The plasma boundary layer, which acts as a virtual anode, and all equipotential planes possess a concave mirror shape.[7] Hence an ion-optical focusing of the extracted ion beam occurs. For an optimum adaption of the extracting voltage, the plasma density, i.e., the transmitter power, and the anchor's geometry, the focus lies exactly in the cathode channel.[6] In this case of optimum focusing the cathode bores can be made very small, whereby the neutral gas losses drop and the mass

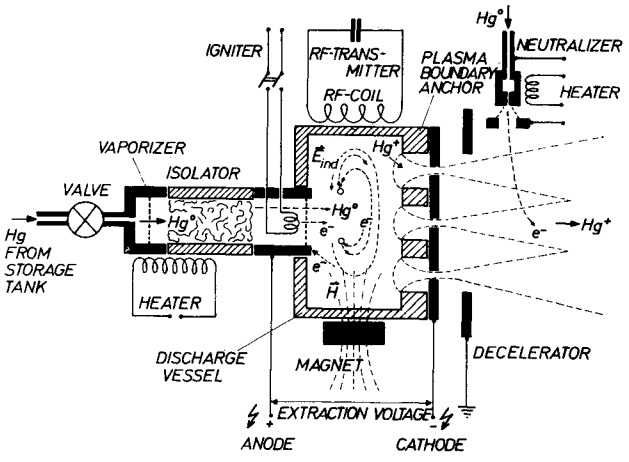

Fig. 1 Scheme of an rf-ion engine.

efficiency of the thruster rises considerably. In the under- or over-focused case, the focal distance is either too long or too short.

The extracted ions are decelerated behind the ion source exit by a grounded decel-electrode to anode potential, i.e., beam voltage. Then the positive jet is neutralized by electron injection from a plasma-bridge neutralizer.

Experimental Work on 10-cm-diam Thrust Units

Preliminary tests indicated an optimum discharge vessel length, nearly equal to the diameter.[4] However, as the measured data scattered, an improved apparatus equipped with a movable glass piston, the position of which could be indicated by a resistance potentiometer has been developed. Without changing any working parameter, the discharge length could be varied continuously during a few seconds. Figure 2 shows one $x - y$-plotter diagram.[8] In accordance with a complete theory and contrary to former conclusions, the optimum length of a 10-cm diam ionizer lies between 2.5 and 3.5 cm. However, it depends on the coil length which should be as short as possible.[8] The optimum frequency of 3.2 MHz, related formerly, has been corroborated. However, the optimum number of turns of the induction coil was found to be 10 instead of 20.

The size, number, position, and polarity of the permanent magnets producing the auxiliary **H**-field also have been optimized. A special apparatus enables rotation of the magnet around the ionizer.[8] Two similar magnets with equal polarity, arranged at 90° to each other, give optimum yield, improving the beam current in respect to a single magnet by 23%.

Former optimizations led to a plasma boundary anchor thickness of 4 mm appropriate for RIT 10, i.e., for specific impulses of 4400 sec. If lower exhaust velocities are desired, the anchor's thickness must be diminished in respect to the

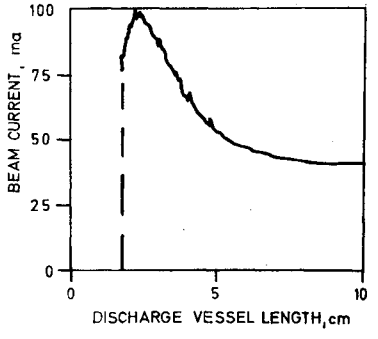

Fig. 2 Optimization of the discharge vessel length (induction coil length: 1.5 cm; number of turns: 6; frequency: 3.2 MHz).

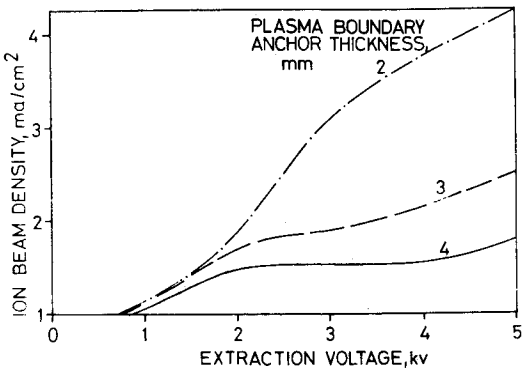

Fig. 3 Influence of the plasma boundary anchor's thickness (parameter) on the extracted ion beam density.

$V^{3/2}$ law. Figure 3 shows the increase of the beam density with decreasing acceleration distance.[8]

We investigated the vaporizer-isolator-system of RIT 10 and calculated and measured the evaporated propellant as a function of the boiler's geometry (i.e., the grid area and the mesh lattice-constant), temperature, and heating power.[9] Figure 4 illustrates the ioslator optimization. A quartz isolator of 12-mm diameter, filled with quartz wool has a breakdown voltage exceeding 10 kv for 200°C.

An 100-hr test of a RIT 10 engine indicated that no working parameters had to be readjusted and that all thruster data remained constant. With the exception of the igniter, which had to be reconstructed, no serious failures occurred. In another one-week continuous run, more than 11,000 start and restart cycles were accomplished without any hangfire or igniter erosion.[4]

Performance of RIT 10

The assembly of a RIT 10 laboratory prototype is shown in Fig. 5. Liquid mercury is fed through the 1-mm-wide propellant pipe into the main vaporizer, made of stainless steel. Its evaporating steel grid has an 78.5 mm² area The 40-mm-long, 12-mm-diam quartz isolator is stuffed with quartz wool. Both vaporizer and isolator are electrically heated to 200°C. The heating element has a minimum power requirement of 3.7 w and is operated at a 6-w level. The isolator is surrounded by an aluminium cylinder for thermal and rf-shielding.

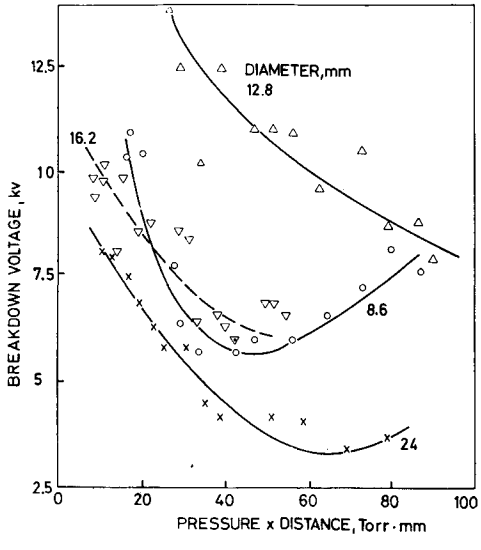

Fig. 4 Paschen graphs in Mercury (isolator length: 4.3 cm; filling: quartz wool of 60 mg/cm³ density).

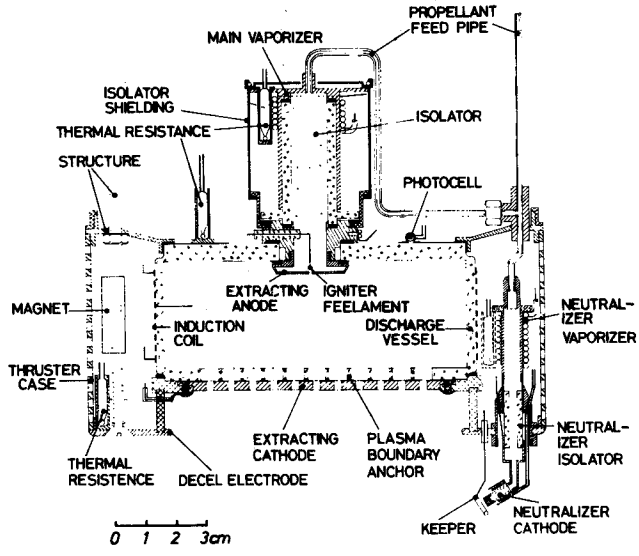

Fig. 5 True scale cross section of the 10-cm rf-ion thruster RIT 10 (see text).

The cylindrical extracting anode acts as propellant inlet. Its bottom is perforated and consists of tungsten. Its potential can be varied from 2.4 to 4.5 kv. In the hollow space of the anode-can, the igniter filament, a thoriated tungsten wire of 0.15 mm diam, is mounted. It is seperated from the discharge plasma by the anode bottom, eliminating all erosion problems. For a filament heating power of 25 w, emission current amounts to about 5 ma. During the ignition time of 0.4 sec, the total igniter's energy consumption does not exceed 22 w sec. After each ignition cycle both filament terminals are disconnected from ground potential.

The 3.5-cm-long, 10-cm-i.d., quartz discharge chamber has a 3-mm-thick wall and a 6-mm-thick lid. On the vessel wall, a silver spiral of 10 turns and 3 cm length is fixed, acting as rf-induction coil. It is connected with the capacitor of the oscillatory circuit and the power transistors, both placed in the electronic and control compartment. The fully transistorized transmitter consumes 47 w and delivers 35 w of rf power.

Two permanent magnets of ferroxdure, 4.5 × 2.5 × 0.75 cm, generate an auxiliary magnetic field of 15 oe average intensity.

Table 1 Mass distribution of the RIT 10 thruster system (kg)

Thruster	Discharge vessel with anchor and coil	0.23	
	Isolator	0.01	
	Main vaporizer	0.04	
	Permanent magnets (2)	0.09	
	Extraction anode with igniter	0.10	
	Extraction cathode	0.24	
	Neutralizer	0.06	
	Case and structure	0.34	
	Subtotal (already optimized)		1.11
Control and electronic unit	Electronic components	0.15	
	Case and structure	0.39	
	Subtotal (optimized)		0.54
High-voltage power conditioning	At present	5.85	
	After optimization		2.30
Total at present		7.50	
Total after optimization			3.95

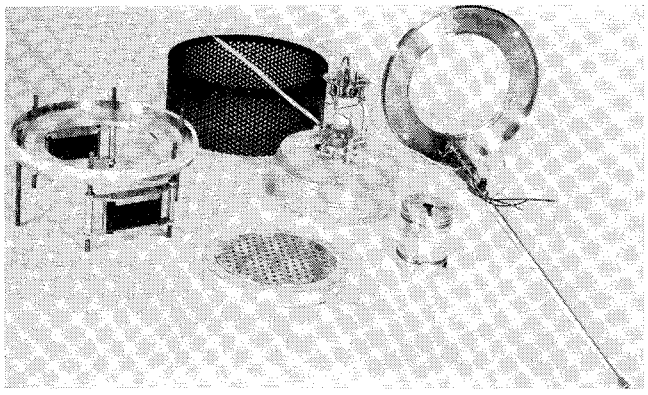

Fig. 6 Disassembled rf-ion thruster RIT 10 (from left to right: structural aluminum ring with 6 threaded bolts and 2 permanent magnets; blacked perforated thruster case; extraction cathode with fiber glass distance ring; discharge chamber with induction coil, isolator, main vaporizer, and Hg feed line; isolator shield; decel electrode with neutralizer and main propellant feed line).

The plasma boundary anchor is made of quartz and melted together with the discharge vessel. It is 4 mm thick and has 121 holes in a hexagonal arrangement, each 6 mm in diameter and coaxial to the 2.5-mm-diam holes of the 3-mm-thick, molybdenum extraction cathode. The cathode potential is adjustable between −0.5 and −3.5 kv, depending on the anode voltage, to maintain the extraction voltage constant between 5 and 6 kv. The cathode drain current amounts to about 1 ma, resulting in an acceleration power loss of 2.6 w.

A grounded, 2-mm-thick steel ring serves as deceleration electode. It carries the plasma bridge neutralizer, consisting of the neutralizer-vaporizer, the isolating through-connections, the heated hollow cathode, and the keeper electrode. The total power consumption of the neutralizer amounts to 13 w.

The thruster case is made of aluminum, perforated in order to avoid heat damming-up; it is 15 cm in diameter, 7 cm long, and 1.5 mm thick. Four thermal resistances and a photocell control the thruster's mode of working.

Figure 6 shows a disassembled RIT 10-engine. The thrust-producing part of the engine is mounted at the bottom of the 10-cm-long control and electronic compartment, which has an axial hollow space to accommodate the main vaporizer-isolator-system. The control compartment contains: 1) the fully transistorized transmitter of the rf-ionizer (47-w d.c.-power input); 2) the power supplies for: the main vaporizer and isolator heater (2.5 v, 6 w), the igniter heater (10v, 25w), the neutralizer-vaporizer (2.5 v, 3 w), the neutralizer cathode heater (10 v, 5 w), and the neutralizer keeper (30 v, 5 w); 3) the power controls for: the transmitter (rf-power range: 10–50 w; power loss: 8 w), the main vaporizer (propellant flow rate range: 0.075–0.3 mg/sec; power loss: 0.6 w), and the neutralizer (electron yield: 30–120 ma; power loss: 1.4 w); 4) the discharge control and automatic igniter switch apparatus; 5) the flash-over guard and high voltage switch-off apparatus; 6) the automatic thruster regulator and face value adjustemnt.

Table 2 Power consumption of RIT 10 components (w)

Transmitter (discharge 35; loss 12)	47	
Isolator and main vaporizer	6	
Accelerator drain current	2.6	
Neutralizer (vaporizer 3; cathode 5; keeper 5)	13	
Total thruster power loss		68.6
Net beam power		240
Pos. high volt. gener. loss	43	
Negat. high volt. gener. loss	0.4	
Control loss (high voltage 32; transmitter 8; vaporizer 0.6; neutralizer 1.4)	42.0	
Total control and power conditioning loss		85.4
Thrust unit gross power input		394

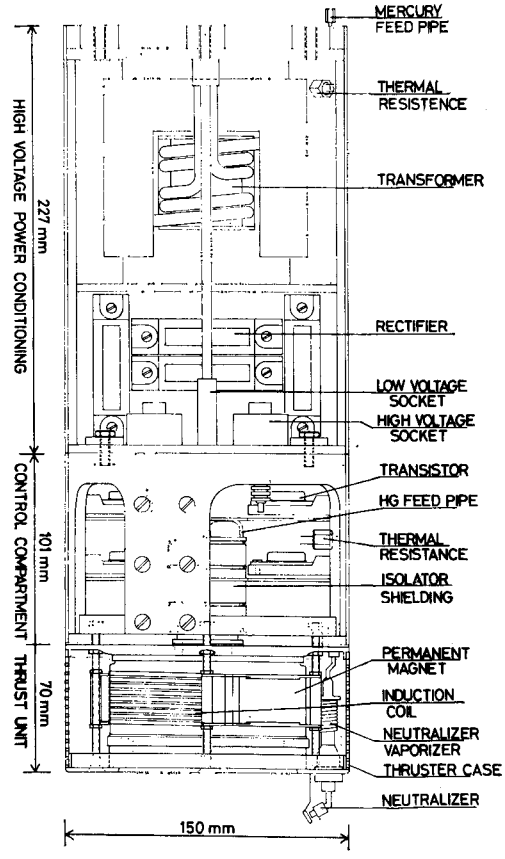

Fig. 7 Cross section true to scale of the RIT 10 thruster system including control and power supply units.

This combined control and electronic compartment is screwed to the high-voltage power conditioning unit (PCU). The cylindrical unit is 22.7 cm long and has the same diameter as the thruster and the control compartments, namely 15 cm. The PCU generates the positive high voltage of the extraction anode (283-w power input, 240-w power output) and the negative cathode voltage (3-w input, 2.6-w output). Both high-voltage generators are regulated and adjusted by a control unit with 318-w power input and 90% efficiency. The unit is being prepared for a mechanical, thermal, and vacuum long-time test and for mass minimizing.

Figure 7 shows a cross section of the totally mounted thrust unit and Fig. 8 a photograph of the 39.8-cm-long RIT 10

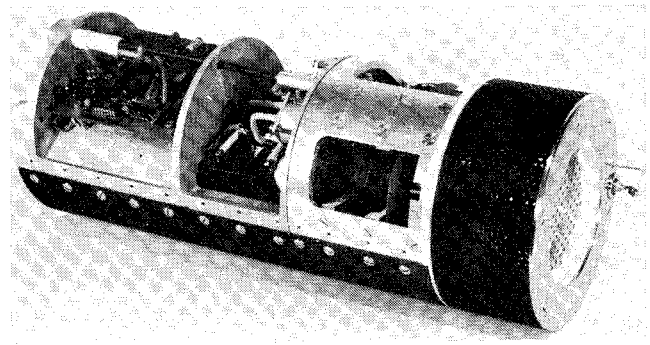

Fig. 8 RIT 10 thruster with control and power conditioning units.

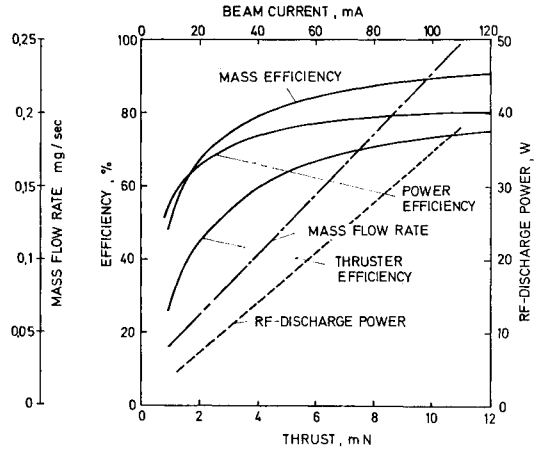

Fig. 9 Thrust variation of a RIT 10 engine.

engine. The mass statement is given by Table 1, while Table 2 shows the power consumption. The most important, standardized RIT 10 thruster performance data are collected in Table 3. In principle, the exhaust velocity of rf-thrusters lies between 20 km/sec and ~200 km/sec. However, in both borderline cases some construction changes must be carried out, e.g., a coating technique is necessary for the lower limit, and on the other border a supplementary acceleration electrode must be installed. For the device shown in Fig. 5, the reasonable beam voltage ranges from 1.5 to 5 kv, resulting in specific impulses of about 3500–6500 sec and thruster efficiencies of 62.5%–80.0%. For changing the specific impulse, the potentials of both extraction electrodes must be shifted by the high-voltage regulator, in equal amounts in order to keep the optimum extraction voltage constant.[10] For varying the thrust level without changing the exhaust velocity, the control and adjusting equipment of the rf-transmitter power, the main vaporizer heater, and of all neutralizer components have to be precisely tuned. Figure 9 shows the dependency of the rf-discharge power, the mass flow rate, and the mass, power, and total thruster efficiencies on the desired thrust, i.e., on beam current.

Space Testing of RIT 10

In 1968, the German Ministry of Scientific Research initiated a feasibility study on a solar-electric propulsion module "SELAM," which was carried out by the firm Bölkow GmbH, Munich.[11] Subsequently, the author made some calculations concerning a spiralling-up mission into an 36,000-km-orbit.[4] After the feasibility and the utility of the first SELAM concept had been proved, the Ministry initiated two advanced concept definition studies. The companies Messerschmitt-Bölkow-Blohm (MBB) and ERNO-Raumfahrttechnik completed their works in December 1969.[12,13] Unfortunately, the original schedule for flight in 1974 has been postponed (due to financial difficulties) probably to 1976.

The major objectives of SELAM are: 1) space testing of the rf-ion drive including variation of thrust and specific impulse; 2) proving the deployment and alignment of large solar panels; 3) integration of solar energy source, power conditioning, propellant distribution and feed systems, control systems, and the thrusters; 4) proving of the cluster technique including variation of thrust vector, engines switch-over tests, and attitude control, and achievement of a high altitude, as an important precursor for subsequent solarelectric missions. Moreover, a SELAM satellite can be used as a Van Allen-probe.

The advanced SELAM studies have established the following specifications[12]: 1) a minimum mission time of 6 months; 2) a starting orbit altitude of 500 km; to guarantee permanent

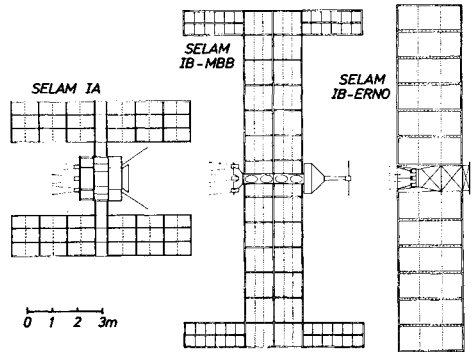

Fig. 10 Comparison of the three SELAM concepts.

sun exposure, a polar orbit is chosen; 3) production of 2.5 kw by the power plant at the beginning of the mission (the solar cells are always sun orientated); 4) a mass and volume (in the folding-up phase) that will permit use of either an improved Thor-Delta (WTR-launch use of place) or an Europe-I-rocket (Kourou, Guiana) as the booster, and 5) six RIT 10 engines to produce a tangential thrust. The maneuverability of the space vehicle must be guaranteed by symmetric engine group operation.

In the first study, the rf-engines were scheduled to work with 65 km/sec resulting in a power requirement of 600 w per engine. Therefore, only 3 thrusters work simultaneously with 45 mN thrust, while the other engines remain in standby.[11] Then, the author calculated the SELAM mission with six RIT 10 units, working together, each with 43.6-km/sec, 10-mN thrust, and 367-w power consumption. The acceleration grew by 34%. The 250-kg satellite could be spiralled up to a 36,000-km orbit during 201 days.[4] The two advanced studies accepted the new thruster working data. However, due to a more conventional panel deployment, the mass increment of the advanced SELAM IB compensates the thrust gain. While the first feasibility study SELAM scheduled a final orbit altitude of 9500 km, the two advanced concepts SELAM IB of MBB and ERNO plan altitudes of 6800 km and 7700 km, respectively. In Table 4 some characteristic mission parameters are collated. Figure 10 shows sketches true to scale of the three SELAM projects.

The design SELAM IA (Fig. 10 left) had an octagonal main body with six RIT 10 engines mounted in a circular arrangement at the top of the structure. The folded-up solar cell array comprised a stiff support, i.e., the main panel, fixed at the satellite core, and orthogonal folding-out, flexible subpanels with a self-hardening plastics structure. The two solar panels, each of 16-m² area, formed an H-shape.

Mechanical and contamination difficulties are avoided by MBB's SELAM IB[12] (Fig. 10 middle). The entire power is

Table 3 RIT 10 performance data

Ion current	100	ma
Mass flow rate ($2.3 \cdot 10^{-4}$ g/sec)	7.4	kg/yr
Beam diameter	8.5	cm
Exhaust velocity	48	km/sec
Specific impulse	4400	sec
Beam power	240	w
Thruster power consumption	309	w
Thrust unit power input	394	w
Beam aperture	12	deg
Thrust	10	mN
Ion production cost	350	ev
Thruster loss per ion	686	ev
Focusing degree (extraction)	99	%
Power efficiency	77.8	%
Propellant efficiency	92	%
Divergence efficiency	99	%
Jet homogeneity	100	%
Total thruster efficiency	70.8	%

Table 4 Typical data of preliminary and advanced SELAM missions

	Initial mass (kg)	Solar panel mass (kg)	Propellant mass (kg)	Number of operational thrusters	Exhaust velocity (km/sec)	Thrust (mN)	mission time (days)	final orbit altitude (km)
SELAM I A Bölkow Ref. 11	250	85	25	3	65	45	180	9,500
SELAM I A Author Ref. 4	250	85	24	6 (4,3,2)	43.6	60	201	36,000
SELAM I B MBB Ref. 12	350	147	27	6 (4,3,2)	43.6	60	180	6,800
SELAM IB ERNO Ref. 13	350	142	22	6 (4,2)	43.6	60	180	7,700

generated by two conventional, stiff clack-out panels. The satellite is divided into three independant, separately testable and exchangeable parts, namely the outfit compartment including telemetry, attitude control, cold-gas tank, and an eventual scientific or commercial payload, secondly the solar cell array, and thirdly the total thruster system including propellant tank, Hg-distribution and feed system, main control unit, power conditioning and thrust engines. The six RIT 10 units are mounted in a circular arrangement with a mutual distance of 37.5 cm. Therefore, suited series of operations of thrusters enable rotations, i.e., attitude control, about any axis that lies in the thruster assembly plane.

The ERNO's SELAM IB device (Fig. 10 right) differs from the latter design by accomodation of all satellite components in the spacing between the two solar panels.[13] A very compact launching assembly resulted. However, it is more difficult to separate the individual components for testing. Moreover, a rectangular, elongated main body and an assembly of the six RIT 10 engines in three pairs, each inclined to a centerline of mass is implicated. This arrangement enables only attitude control in respect to one axis. Furthermore, the removed position of the thrust engines run the risk of mercury contamination of the solar cells.

Variation of Thruster's Size

We investigated scaling laws of rf-ion sources from 4 to 10 cm diam.[14] Figure 11 gives some results of the ionizer optimization measurements. As it has been predicted theoretically,[4] both the optimum discharge pressure and the optimum rf-frequency rised inversely proportional to the vessel radius. The beam density yield, i.e., the ion current per extraction hole divided through the discharge power, seems to drop slightly with ionizer's size. Concerning the optimum magnetic field and the optimum coil turn number, there has been found no striking relationship to the ion source diameter. The number of extraction holes raised from 7 to

Table 5 Predicted properties of RIT 4 and RIT 20 in comparison to RIT 10

	RIT 4	RIT 10	RIT 20
Optimum discharge pressure, torr	2.10^{-3}	2.10^{-4}	7.10^{-5}
Optimum magnetic field, oe	15	12	10
Optimum transmitter frequency, MHz	9	3.2	1.3
Transmitter power, w	15	47	150
Ion current, ma	12	100	450
Ion production costs, ev	940	350	250
Thrust, mN	1.2	10	45
Thrust power input, w	50	309	1,350
Power efficiency, %	60	77.8	84
Thruster efficiency, %	45	70.8	79

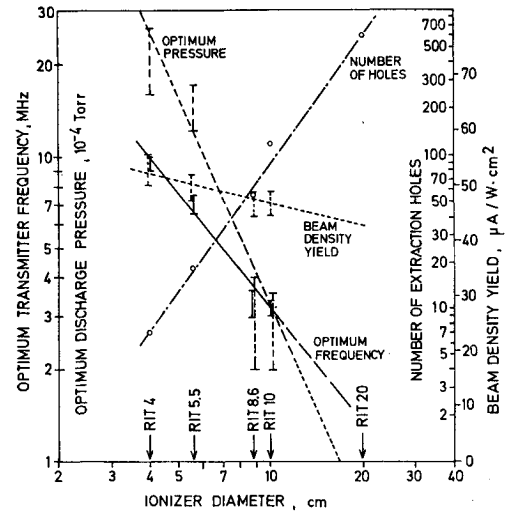

Fig. 11 Scaling laws of optimized rf-thruster performance data.

121 (with unchanged anchor and cathode geometry and constant extraction voltage).

After having determined all optimum parameters (including the discharge vessel length and the extraction system), the 4-cm thrust unit will be developed to prototype maturity comprising power conditioning, thruster control, propellant feed system, vaporizer, isolator, and neutralizer. Table 5 gives some predicted performance data. Six RIT 4-engines would be suitable for attitude control and station keeping of synchronous satellites weighting 2 or 3 tons for a mission time of 3–5 yr.

In order to develop a main propulsion rf-engine, the scaling laws for enlargement the RIT 10-ionizer in three steps, to 20-cm, 35-cm, and 50-cm-diam ion sources, will be investigated.

At present, first optimizations of RIT 20 are running. The discharge vessel is 8 cm long and 20 cm in diameter. The ion extraction system has 595 borings. The anchor and cathode hole's geometry is the same as of RIT 10. Table 5 gives some predicted data of RIT 20, too. The RIT 50-engine is scheduled for 2.5-a ion current. Four or six RIT 50 can be used for spiralling-up 2-ton satellites or as main propulsion system of interplanetary probes.

The optimization measurements of all thrusters larger than 10-cm diam (as well as the RIT 10-cluster experiments) are performed in a new large vacuum facility of 28-m³ volume and 100,000 liter/sec pumpting speed.

References

[1] Loeb, H. W., "Ein elektrostatisches Raketentriebwerk mit Hochfrequenzionenquelle," *Astronautica Acta*, Vol. 8, No. 1, Jan. 1962, pp. 49–62.

[2] Freisinger, J. and Loeb, H. W., "Optimierung des Giessener Ionentriebwerkes," *Raumfahrtforschung*, Vol. 10, No. 4, Oct. 1966, pp. 174–179.

[3] Loeb, H. W., "Verwendungsmoeglichkeit der Hochfrequenzionenquelle in elektrostatischen Raketentriebwerken," *Zeitschrift fuer angewandte Physik*, Vol. 26, No. 3, March 1969, pp. 245–254.

[4] Loeb, H. W., "State of the Art and Recent Developments of the Rf-Ion Motors," AIAA Paper 69-285, Williamsburg, Va., 1969.

[5] Pfeiffer, B., "Der Skineffekt bei anisotropen Plasmen mit besonderer Beruecksichtigung von Resonanzerscheinungen im induktiv erregten Hochfrequenzplasma," *Mitteilungen aus dem Institut fuer Hochfrequenztechnik an der ETH Zurich*, 1st ed., Vol. 1, Juris-Verlag, Zurich, 1965, pp. 5–89.

[6] Freisinger, J., Groh, K., and Loeb, H. W., "Extraction and Acceleration Mechanism in Rf-Ion Thrusters," AIAA Paper 69-284, Williamsburg, Va., 1969.

[7] Reifenschweiler, O., "Aehnlichkeitsgesetze bei Hochfrequenzionenquellen," *Annalen der Physik*, Vol. 14, No. 6, June 1954, pp. 33–40.

[8] Klein, W., "Optimierungen an einer Hochfrequenzionenquelle von 10 cm Durchmesser," Diploma thesis, March 1970, 1st Institute of Physics, Univ. of Giessen.

[9] Koschade, S., "Zur Massenbilanz einer Hf-Ionenquelle," Diploma thesis, April 1970, 1st Institute of Physics, Univ. of Giessen.

[10] Freisinger, J. and Loeb, H. W., "Auslegungsgroessen von Hf-Ionentriebwerken fuer Raumtests," *Raumfahrtforschung*, Vol. 13, No. 4, July 1969, pp. 149–156.

[11] "Solarelektrisches Antriebsmodul SELAM," *Feasibility study*, Aug. 1968, Bölkow, GmbH., Ottobrunn-Munich.

[12] "Solarelektrisches Antriebsmodul SELAM," *Concept definition study*, Dec. 1969, Messerschmitt-Bölkow-Blohm GmbH., Ottobrunn-Munich.

[13] "SELAM," *Concept definition study*, Dec. 1969, ERNO Raumfahrttechnik GmbH., Bremen.

[14] Trojan, F., "Aehnlichkeitsgesetze bei kleinen Hf-Ionentriebwerken," Doctorate thesis, 1971, 1st Institute of Physics, Univ. of Giessen.

MAY 1971 J. SPACECRAFT VOL. 8, NO. 5

NERVA Technology Reactor Integrated with NASA Lewis Brayton Cycle Space Power Systems

L. H. BOMAN* AND J. G. GALLAGHER†
Westinghouse Astronuclear Laboratory, Pittsburgh, Pa.

A conceptual design of this 2.2 Mw reactor has been performed to permit integration with power conversion units which are in an advanced state of development. The reactor has flexibility for application with 25 to 600 kwe space power systems. Design concepts and methods utilized were developed in the NERVA program. Uranium bearing graphite fuel elements, utilizing fuel particles developed for commercial power reactors, form a cylindrical core, reflected radially, and at the inlet end by beryllium. It is controlled by rotating control drums located in the radial reflector. A manned space-base system design concept, including shielding analysis, is also discussed.

Introduction

WESTINGHOUSE Astronuclear Laboratory has engaged in a design study of a high-temperature space power reactor for application in a Brayton cycle space electric power system. A 1-Mw version of this reactor has been reported.[1] The reactor has been designated "The NERVA Technology Reactor" (NTR) because it utilizes the proven design concepts and design methods developed in the NERVA (Nuclear Engine for Rocket Vehicle Application) program. This report presents the conceptual design of the 2.2 Mwt reactor integrated with Brayton cycle power conversion systems under development at the NASA Lewis Research Center. This reactor has the flexibility for application over a range of thermal power providing electric power requirements from 25 kwe to 600 kwe. Two applications are considered: one for the 100-kwe power requirement of the manned space base,[2] and one to provide 506 kwe at the reactor design point of 2.2 Mwt for 50,000 hr at 1600°F exit gas temperature.

Received October 1, 1970; presented as AIAA Paper 70-1226 at the AIAA 7th Annual Meeting and Technical Display, Houston, Texas, October 19–22, 1970; revision received February 17, 1971. This work was performed under a Company funded study. Comments and suggestions given by members of the staff of the Lewis Research Center of NASA on a draft of the design study which is summarized in this paper are gratefully acknowledged. The permission received to abstract material from the NASA Lewis internal memorandum[6] is also acknowledged.

* Supervisor, Core Thermal Design, NERVA Project.
† Manager of Design Engineering, NERVA Project. Member AIAA.

Since 1963, The NASA Lewis Research Center has carried on a closed Brayton-cycle component and power system development program. Favorable long-duration test experience has been accumulated on a 15-kwe power system, and on individual components of this system, while a 160-kwe system is in the initial hardware design phase. For this application, these power conversion units are in a direct gas loop with the reactor.

The NERVA technology is a broad-base highly-developed technology covering all reactor engineering and systems technology. This nuclear rocket program started by the Los Alamos Scientific Laboratory in 1955 has been marked since 1964 by ground tests of 12 reactors at unprecedented power density and temperature levels. Reference 3 presents a summary of the NERVA program. The use of an inert gas in the direct reactor Brayton cycle space power system permits the NTR to operate for the extended duration required. Both the NERVA reactor and the NTR are gas-cooled beryllium reflected reactors utilizing graphite dispersion uranium carbide fuel and controlled by rotating control drums in the radial reflector.

Several operating and planned central station gas-cooled power reactors utilize fuel similar to that required for this space power application. Some of these, or their prototypes, have been built (HTGR, AVR, DRAGON, and UHTREX), while others are still under construction (Ft. St. Vrain and THTR).[4] The requirements for fuel performance in these graphite dispersion fueled reactors are nearly identical to those of the reactor-Brayton system application. The fuel has the required excellent fission product retention at the temperatures, burnup, power rating, irradiation levels, and lifetime needed for this space electric power system.[5]